HERIOT WATT UNIVERSITY

Heriot-Watt University
Research Gateway

Deciphering the mechanism of the nickel-catalyzed hydroalkoxylation reaction

Citation for published version:
Mifleur, A, Mérel, DS, Mortreux, A, Suisse, I, Capet, F, Trivelli, X, Sauthier, M & Macgregor, SA 2017, 'Deciphering the mechanism of the nickel-catalyzed hydroalkoxylation reaction: A combined experimental and computational study', *ACS Catalysis*, vol. 7, no. 10, pp. 6915-6923.
https://doi.org/10.1021/acscatal.7b00616

Digital Object Identifier (DOI):
10.1021/acscatal.7b00616

Link:
Link to publication record in Heriot-Watt Research Portal

Document Version:
Peer reviewed version

Published In:
ACS Catalysis

Publisher Rights Statement:
This document is the Accepted Manuscript version of a Published Work that appeared in final form in ACS Catalysis, copyright © American Chemical Society after peer review and technical editing by the publisher. To access the final edited and published work see http://pubs.acs.org/doi/10.1021/acscatal.7b00616

General rights
Copyright for the publications made accessible via Heriot-Watt Research Portal is retained by the author(s) and / or other copyright owners and it is a condition of accessing these publications that users recognise and abide by the legal requirements associated with these rights.

Take down policy
Heriot-Watt University has made every reasonable effort to ensure that the content in Heriot-Watt Research Portal complies with UK legislation. If you believe that the public display of this file breaches copyright please contact open.access@hw.ac.uk providing details, and we will remove access to the work immediately and investigate your claim.

Download date: 05. May. 2023

Deciphering the mechanism of the nickel-catalyzed hydroalkoxylation reaction: A combined experimental and computational study.

Alexis Mifleur,† Delphine Merel,† André Mortreux, † Isabelle Suisse, † Frederic Capet,† Xavier Trivelli,# Mathieu Sauthier,*, † Stuart A. Macgregor.* ‡

† Univ. Lille, CNRS, Centrale Lille, ENSCL, Univ. Artois, UMR 8181 - UCCS - Unité de Catalyse et Chimie du Solide, F-59000 Lille, France

‡ Institute of Chemical Sciences, Heriot-Watt University, Edinburgh, EH14 4AS, UK

Université de Lille, CNRS, UMR 8576, UGSF, Unité de Glycobiologie Structurale et Fonctionnelle, 59000 Lille, France

ABSTRACT: The [Ni(0)(cod)$_2$]/P⌒P-catalyzed hydroalkoxylation of butadiene to form butenyl ethers is studied mechanistically, where P⌒P = 1,4-bis(diphenylphosphino)butane (dppb) and 1,2-bis(diphenylphosphinomethyl)benzene (dppmb). Experimental studies suggest the intermediacy of [(P⌒P)Ni(0)(butadiene)] and [(P⌒P)Ni(II)(allyl)] intermediates and rule out the involvement of Ni-H species. The related species [(dppb)Ni(0)(1,4-diphenylbutadiene)], **1**, and [(P⌒P)Ni(II)(crotyl)(Cl)] complexes **2** (P⌒P = dppmb) and **3** (P⌒P = dppb) have been synthesized and characterized on the basis of VT NMR spectroscopy and X-ray crystallographic studies. **2** and **3** are shown to be catalytically competent for the hydroalkoxylation reaction. Computational studies on [(dppmb)Ni(0)(butadiene)] indicate a facile protonation that forms a cationic allylic intermediate [(dppmb)Ni(II)(η-C$_4$H$_7$)]OMe. C-O bond formation then occurs via external attack by the solvent-stabilized methoxide nucleophile. Hydroalkoxylation proceeds with modest computed barriers of ca. 18 kcal/mol and the butenyl ether product formation is only marginally exergonic. Overall the results are consistent with initial kinetic control leading to the major branched isomer followed by a reversible isomerization process operating under thermodynamic control.

KEYWORDS (Word Style "BG_Keywords"). Hydroalkoxylation, butadiene, nickel, mechanism, allyl

INTRODUCTION

The formation of carbon-heteroatom bonds is crucial in organic chemistry to provide new molecular scaffolds, and realizing this in catalytic processes is particularly desirable, especially if they occur under mild conditions and with high stereoselectivity.[1] The construction of C-O bonds in O-alkyl or -allyl ethers has traditionally used the Williamson reaction. However, this process necessarily results in stoichiometric salt formation, and may also give unwanted organic side-products. The development of atom economic catalytic methods that reduce waste and so better fulfill the criteria of green chemistry is therefore of great interest.[2]

One such process is the transition metal-mediated formation of ethers via the hydroalkoxylation reaction – the addition of the O-H bond of an alcohol over a C=C double bond. Using butadiene and alcohols in the presence of transtion metal catalysts generally results in the so-called telomerization reaction, where the C-O bond is formed after a previous C-C coupling of two butadiene units, allowing an efficient access to octadienyl ethers. [3] First observed during butadiene dimerization in the presence of nucleophiles[4] this reaction is efficiently promoted using low catalyst loadings of palladium salts in the presence of phosphines[5] or carbene[6] ligands. Butadiene telomerization is important industrially as it provides access to higher value intermediates such as 1-octene and octanol,[7] as well as surfactants via association of the C8 lipophilic chains with hydrophilic polyols.[8] Although C8 telomers are the major products, higher telomers containing three to six butadiene units can also be formed,[9] for example with cationic (η^3-allyl)palladium catalysts mixtures containing C8, C16 and C24 telomers are observed.[10]

The direct hydroalkoxylation of butadiene, also known as degenerative telomerization, results in C4 butenyl ethers. The first selective synthesis of butenyl ethers was reported by Dewhirst via the reaction of butadiene in ethanol in the presence of high loadings of $RhCl_3$.[11] Smutny et al. observed the hydroalkoxylation of butadiene with phenol by using π-allylpalladium-based catalysts. However the reaction suffered from low yields and the formation of significant amounts of by-products.[12] Subsequently the use of chelating phosphines with strongly electron donating substituents gave improved selectivities. Similarly, the combination of basic monodentate trialkylphosphines, PR_3 (R = Et, ^{n}Bu), with π-allylpalladium(II) chloride dimer precursors provided selective butadiene hydroalkoxylation, as long as the reaction was performed under high methanol dilution conditions.[13]

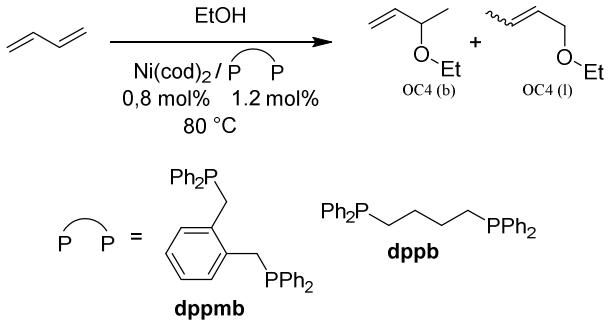

Scheme 1. Ni-catalysed butadiene hydroalkoxylation.

The few available reports on the related nickel-catalysed reactions of 1,3-butadiene generally indicate lower efficiencies for both the hydroalkoxylation and the telomerization processes.[14] In contrast, our group has recently reported that the hydroalkoxylation reaction can be achieved with both high butadiene conversion and high selectively when using a catalytic system featuring zero-valent nickel in the presence of chelating phosphines (Scheme 1).[15] The structure of the ligand has a strong bearing on the reaction outcome. Thus, no reaction was observed with either 1,2-bis(diphenylphosphino)ethane (dppe) or 1,3-bis(diphenylphosphino)propane (dppp). However, ligands with four carbon backbones such as 1,4-bis(diphenylphosphino)butane (dppb) and 1,2-bis(diphenylphosphinomethyl)benzene (dppmb) promote the selective formation of butenyl ethers that are obtained as mixtures of the branched (b) and linear (l) isomers. Using monodentate phosphines only led to linear butadiene dimerization. The allylic structures of the branched or linear ethers formed in this hydroalkoxylation reaction - and the lack of any 4-alkoxybut-1-ene products - strongly support the involvement of π-allylnickel intermediates rather than a direct nucleophilic attack on the diene. However, the mechanism by which such species are formed from an alcohol and butadiene remains unclear. In this work, we present a combined experimental and computational study that aims to elucidate the mechanism of the butadiene hydroalkoxylation reaction with nickel catalysts in the presence of chelating phosphines.

RESULTS AND DISCUSSION

π-allylnickel species are usually obtained from the reaction of butadiene with a nickel hydride, where the latter is typically generated via protonation of a Ni(0) precursor (*Path A*, Scheme 2).[16] The formation of such Ni-H intermediates under acidic conditions has been exploited in the dimerization[17] or hydroamination reactions of dienes.[18]

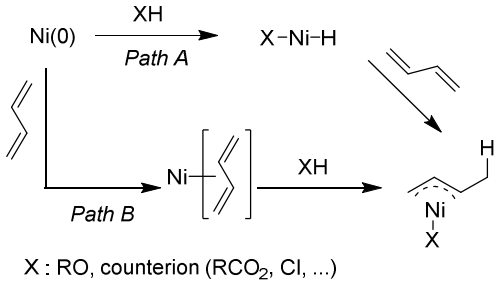

Scheme 2. Pathways to π-allylnickel intermediates from butadiene.

A Ni-H pathway has been also postulated under neutral conditions for the addition of terminal alkynes to 1,3-butadiene.[19] In this case, it is proposed that a Ni-H intermediate forms via oxidative addition of the terminal C-H bond of the alkyne at a Ni(0) precursor. Evidence for the intermediacy of a Ni-H species in the current hydroalkoxylation reactions was sought by performing catalytic reactions in ethanol in the presence of catalytic amounts of acids or bases (Table 1).

Entry	additives (eq./Ni) [b]	Conv. [c] (%)	OC4 [c] (%)	b/l ratio [d]	OC8 [c] (%)	C8 [c] (%)
1	None	20	91	5.9	4	5
2	H_2O (10)	18	93	3.1	3	4
Acids						
3	AcOH (1)	0	0	-	0	0
4	TFA (1)	0	0	-	0	0
5	$MeSO_3H$ (1)	0	0	-	0	0
6	NH_4BF_4 (1)	0	0	-	0	0
7	$B(OH)_3$ (10)	5	88	3.8	3	9
bases						
8	Et_3N (1)	20	91	5.3	4	5
9	Cs_2CO_3 (1)	20	91	4.9	5	4
10	EtONa (1)	24	92	5.3	6	3
11	EtONa (10)	30	94	4.9	4	3
12	KOH (1)	25	92	5.3	4	4

[a]Reaction conditions: Butadiene = 1.5 mL (17.2 mmol); BD/[Ni(0)$(cod)_2$]/ligand: 1250/1/1.5; ROH/BD = 10; Toluene = 3 mL; T = 80°C; t = 30 min. [b] Number of equivalents of additive / amount of nickel. [c] Determined by GC using heptane as an internal standard – selectivities in butenyl ethers (OC4), products of telomerization (OC8) and products of dimerization (C8). [d] b/l = branched / linear ratio for OC4 ethers.

Table 1. Acids/bases additives for butadiene hydroalkoxylation with ethanol.[a]

Short reaction times were employed as incomplete conversions allow for a more straightforward comparison between the different reaction conditions. The presence of acids clearly inhibits the catalytic reaction, with no conversion of butadiene observed with a large scope of acids (entries 3 – 6). Only boric acid allows some conversion (entry 7), albeit still lower than under additive-free conditions (entry 1). Water doesn't lead to any noticeable changes (entry 2). In contrast, the hydroalkoxylation reaction does prove compatible with the presence of bases. Thus Et_3N and Cs_2CO_3 (entries 8 – 9) have no effect on either butadiene conversion or product selectivity, while stronger bases such as hydroxide or alkoxides actually give slightly higher yields (entries 10 – 12). Interestingly in the context of this mechanistic study, the nature of the solvent showed an important effect on both the conversion of 1,3-butadiene and the chemoselectivity of the reaction (Table 2). Starting with the same reactions conditions as table 1 but after longer reaction time (3 h) the conversion of 1,3-butadiene reaches 75 % along with a very comparable selectivity towards OC4 ethers (compare entry 1 of table 1 with entry 1 of table 2). However, by decreasing the ethanol / toluene ratio from 10 mL / 3 mL to 1 mL / 12 mL, the conversion of butadiene dramatically drops. Moreover, the selectivity in products of butadiene dimerization (C8) increases up to 93 % with an ethanol / toluene ratio of 1 mL / 12 mL.

Entry	Solvent Ethanol / toluene (mL / mL)	Conv. (%)[b]	OC4 (%)[b]	OC8 (%)[b]	C8 (%)[b]
1	10 / 3	75	95	2	3
2	6.5 / 6,5	25	78	4	18
3	1 / 12	8	5	2	93

[a]Reaction conditions: Butadiene = 1.5 mL (17.2 mmol); BD/[Ni(cod)$_2$]/ligand: 1250/1/1.5; Toluene = 3 mL; T = 80°C; t = 3 hours. [b] Determined by GC using heptane as an internal standard – selectivities in butenyl ethers (OC4), products of telomerization (OC8) and products of dimerization (C8) - the l/b ratio are very similar in the three experiments.

Table 2. Solvent effect on butadiene hydroalkoxylation with ethanol.[a]

The basic conditions are inconsistent with the formation of a Ni-H intermediate and indicate that another activation mode must be considered. One such possibility is the direct reaction of an alcohol with a Ni(0) species coordinated by a butadiene ligand (*Path B*, Scheme 2), as suggested by Jolly in the case of palladium catalysis.[20] To assess whether this pathway may also operate for nickel, the synthesis of [(dppb)Ni(0)(butadiene)] was attempted from the reaction of [Ni(0)(cod)$_2$] (cod = 1,5-cyclooctadiene) with one equivalent of phosphine and an excess of 1,3-butadiene at room temperature. Unfortunately this complex, if formed, proved to be extremely unstable and could not be unambiguously characterized. We attribute this low stability to the high volatility of butadiene and its facile, irreversible dissociation from the Ni center under vacuum during workup. Instead the related Ni complex **1** was prepared using the high boiling point model substrate, 1,4-diphenyl-1,3-butadiene, via ligand exchange with [Ni(cod)$_2$] in the presence of dppb in toluene (Scheme 3).

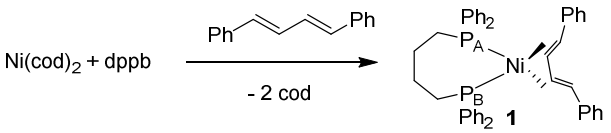

Scheme 3. Synthesis of [(dppb)Ni(0)(1,4-diphenylbutadiene)], 1.

As expected, Ni(0) compound 1 showed a high air sensitivity due to diene lability and facile metal oxidation by O_2. However, 1 could be isolated and fully characterized by spectroscopic methods in the presence of a slight excess of 1,4-diphenylbutadiene. The room temperature ^{31}P NMR spectrum shows a broad singlet at δ 29.3 ppm corresponding to two equivalent phosphorus atoms (Figure 1). The ^{13}C NMR spectrum of the complex shows shielded signals for the diene carbons at 82.4 ppm and 89.6 ppm (129.7 ppm and 133.2 ppm for the free ligand), thus evidencing the coordination of all four carbon atoms of the diene to the metal. A coalescence/decoalescence phenomenon is observed through a variable temperature study ranging from 293 K to 200 K (Figure 1). The broad singlet initially observed in the ^{31}P NMR spectrum at room temperature disappears at 240 K and subsequently re-emerges as two new doublets at δ 20.8 ppm and δ 41.7 ppm ($^2J_{P\text{-}P}$ = 30 Hz) at 220 K that correspond to two inequivalent phosphorus atoms. On the other hand, the low temperature (200 K) ^{13}C NMR spectrum still exhibits only two signals corresponding to the four carbons of the diene moiety. This feature is consistent with the *cis* coordination of the η^4-diene coordinated to the metal which is undergoing a rapid dynamic equilibrium involving diene inversion (Figure 1), similar to that reported in [($Cy_2PCH_2CH_2PCy_2$)Ni(0)(η^4-butadiene)][21] and [($Pr^i_2PCH_2CH_2PPr^i_2$)Ni(0)(η^4-isoprene)].[22]

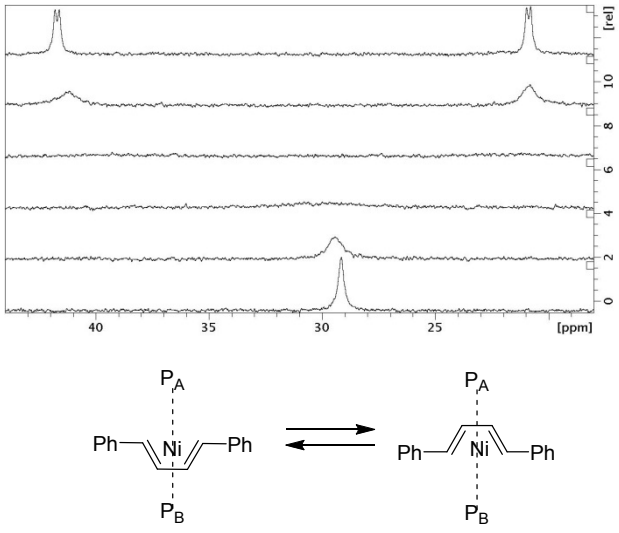

Figure 1. Coalescence/decoalescence phenomena of [(dppb)Ni(1,4-diphenylbutadiene)] observed in ^{31}P-NMR at 162 MHz; from bottom to top: 293, 280, 260, 240, 220 and 200 K.

The inversion process involves nickel intermediates with a η^2-diene and it is noteworthy that both η^2- and η^4-coordination modes of a diene have been observed in [(diphosphine)nickel(0)] complexes.[22] Interestingly, despite its limited

stability, **1** can be used as a catalyst precursor for the hydroalkoxylation reaction. The assumption that π-allylnickel(II) species are intermediates in the Ni-catalyzed reaction prompted us to synthesize the related chloride adducts [(P⌒P)Ni(II)(C_4H_7)Cl], (P⌒P = dppmb, **2** or dppb, **3**) to study their reactivity. **2** and **3** can be prepared either via reaction of [(crotyl)Ni(II)Cl]$_2$ [23] with P⌒P or via the direct reaction of [Ni(0)(cod)$_2$] with 1 equiv of P⌒P and 3 equiv of crotylchloride.

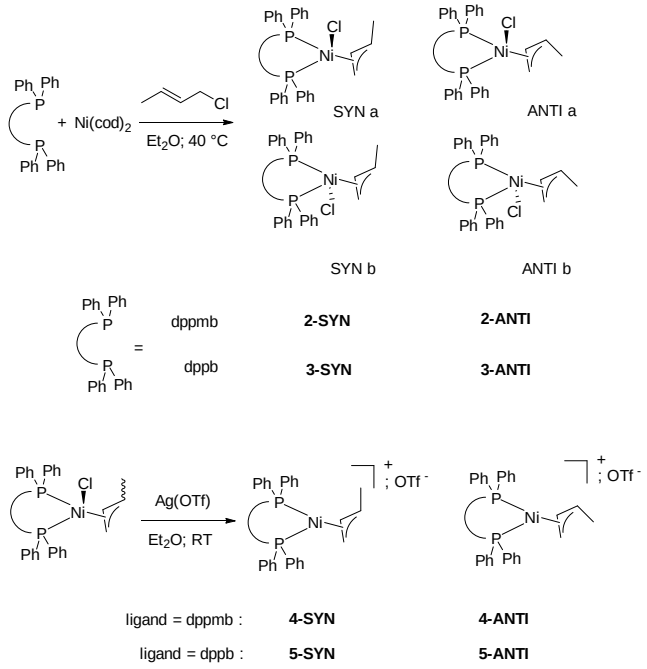

Scheme 4. Synthesis of [(P⌒P)Ni(crotyl)Cl] and [(P⌒P)Ni(crotyl)$^+$]; OTf$^-$ complexes – possible isomeric structures.

Four isomeric structures for **2** and **3** can be envisaged (see Scheme 4), although NMR data suggest that only one SYN and one ANTI isomer is obtained in solution in each case. We cannot determine which of these isomers (i.e. SYN a *vs.* SYN b and ANTI a *vs.* ANTI b) is present. Both **2** and **3** exhibit fluxional behavior, as evidenced by the presence of broad signals at 300 K in both the ^{1}H and ^{31}P NMR spectra. The SYN and ANTI structures of the allylic moieties were unambiguously determined by NOESY experiments. According to the integration of the ^{1}H NMR resonances obtained for the CH_3 groups, the SYN/ANTI ratio is 75/25 in **2** and 50/50 in **3**. It is noteworthy that the two isomers (SYN and ANTI) in complex **2** are not in equilibrium with each other as no correlation is observed in the NOESY spectrum between the two methyl groups of the allylic moiety.

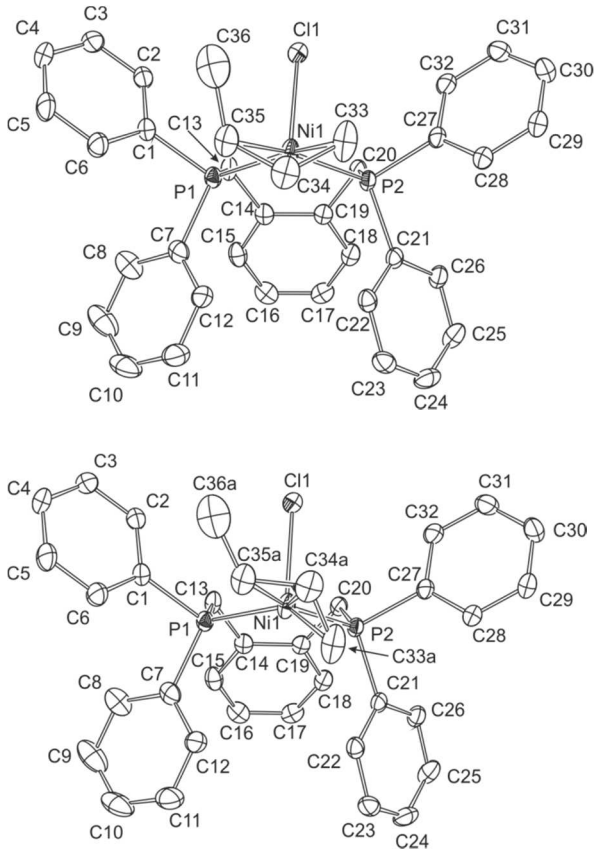

Figure 2. X-ray diffraction study of [(dppmb)Ni(II)(crotyl)Cl], complex **2 (**upper: ANTI isomer; lower: SYN isomer).

Thermal ellipsoid plots are at the 50% probability level. Hydrogen atoms and solvent are omitted for clarity. Selected bond lengths (Å) and angles (deg), ANTI isomer: Ni1-P1 = 2.2148(5), Ni1-P2 =2.1927(5), Ni1-C33 = 2.055(4), Ni1-C35 = 2.075(5), Ni1-C34 =1.986(3), Ni1-Cl1 = 2.4371(5), C33-C34 = 1.418(6), C34-C35 =1.431(7), C35-C36 = 1.568(15); Cl1-Ni1-P1 = 92.472(19), Cl1-Ni1-P2 = 88.678(18), P2-Ni1-P1 = 103.69(2); SYN isomer (where only the position of the allylic carbons differ from the ANTI isomer): Ni1-C33A = 2.032(8), Ni1-C35A = 2.115(13), Ni1-C34A =2.047(6), C33A-C34A = 1.372(13), C34A-C35A =1.403(14), C35A-C36A = 1.47(3).

Suitable crystals for X-ray diffraction studies on complexes **2** and **3** have been grown (Figure 2 and Figure 3). For complex **2** these showed the presence in the crystal of two isomers which differ in the conformation of the allylic moiety. In one case, the methyl is in a SYN position whereas in the other case the methyl is located on the ANTI position (see Figure 2). In both structures, complex **2** features square-pyramidal coordination at nickel with chloride in an axial position. This geometry is comparable to related nickel methylallyl complexes [(dippe)Ni(II)(CH_2CHCH_2)(Br)] (dippe = 1,2-bis(diisopropylphosphino)ethane) and [(dippe)Ni(II)(CH_2CHCH_2)(CN)].[24] The geometry of **2** however differs significantly from that of [(dppb)Ni(II)($CH_2CHCHCH_3$)(CN)] which exhibits a more pronounced trigonal-bipyramidal geometry with the methylallyl in an axial position.[25] Complex **3** exhibits a similar geometry to **2**. Both chelating phosphine ligands in **2** and **3** show

similar bite angles of 103.69(2)° and 100.35(3)°. Although the NMR data for complex **3** clearly show the presence of both the SYN and ANTI isomers in solution, only the SYN isomer was obtained in the X-ray diffraction study.

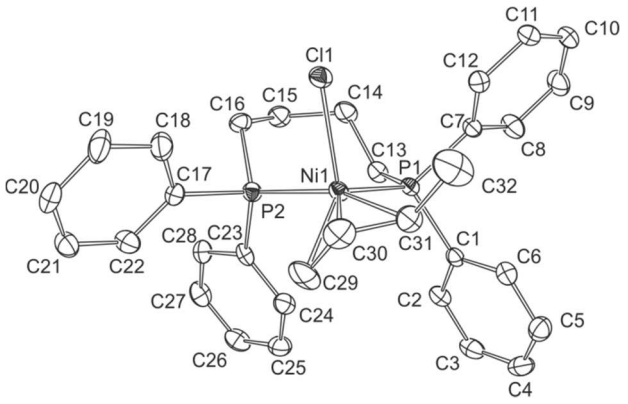

Figure 3. X-Ray diffraction study of [(dppb)Ni(II)(crotyl)Cl], complex **3**.

Thermal ellipsoid plot are at the 50% probability level. Most hydrogen atoms and solvent are omitted for clarity. Selected bond lengths (Å) and angles (deg): Ni1-P1 = 2.2207(7), Ni1-P2 =2.1990(7), Ni1-C29 = 2.054(3), Ni1-C30 = 1.994(3), Ni1-C31 =2.114(3), Ni1-Cl1 = 2.4012(7), C29-C30 = 1.363(4), C30-C31 =1.497(4), C31-C32 = 1.497(4); Cl1-Ni1-P1 = 106.27(3), Cl1-Ni1-P2 = 92.78(3), P2-Ni1-P1 = 100.35(3).

The cationic nickel(II) complexes **4** and **5** were respectively obtained from the complexes **2** and **3** through chloride abstraction with AgOTf in ether at room temperature (Scheme 4). The ^{1}H and ^{31}P NMR spectra in CD_2Cl_2 at low temperature evidenced the presence of a mixture of one ANTI and one SYN isomers. According to the integration of the ^{1}H NMR resonances obtained for the CH_3 groups, the SYN/ANTI ratio is 65/35 for **4** and 80/20 for **5**. Similarly to the neutral complexes, variable ^{1}H NMR studies evidenced a fluxionality due to allyl inversion with both cationic complexes **4** and **5**.

Complexes **2** and **3** can be used as catalyst precursors, providing that a base is added to the reaction medium (Scheme 5). Thus complex **3** does not catalyze the hydroalkoxylation of butadiene in neat ethanol under standard catalytic conditions. However, addition of 10 equiv. of NaOEt (relative to nickel) initiates catalysis with the formation of butenyl ethers at a reaction rate and selectivity (b:l ratio) that are similar to those obtained from the direct use of the [Ni(0)(cod)$_2$]/dppb system. The cationic complexes [(P⌒P)Ni(crotyl)]$^{+}$; OTf^{-} showed a similar behavior and complex **5** was not active under the same catalytic conditions while high conversion were obtained with sodium ethoxide as additive (Scheme 5). The selectivities compare well with the results obtained from the neutral complex **3** thus suggesting that similar intermediates are involved. Noteworthy, the stoichiometric reaction of the complex **3** with NaOEt in ethanol at room temperature also leads to the fast formation of the butenyl ethers and the isomeric composition of the products compares well with that obtained after a catalytic run (Scheme 5). A ^{31}P NMR spectrum of the reaction medium showed the rapid formation of [Ni(0)(dppb)$_2$] as major Ni-containing species.

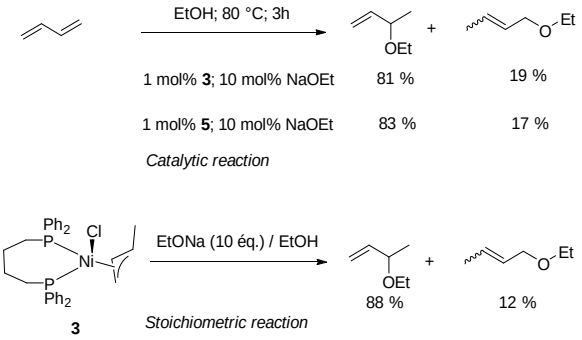

Scheme 5. Reactivity of complex 3 and 5.

Complementary experiments showed that this hydroalkoxylation reaction is reversible at the temperature used for catalysis (80°C). Thus, the reaction of a butenyl ethyl ether mixture containing an enantio-enriched branched isomer (70 % e.e.)[i] with ethanol as reactant and in the presence of the achiral [Ni(0)(dppb)$_2$] catalyst leads to a full racemization within 3 hours at 80 °C (Scheme 6). In addition to the racemization, it is noteworthy that the isomeric mixture is also modified; the b:l ratio is decreased from 72:28 to 50:50.[26] The reversibility was also evidenced from a trans-etherification reaction. For this purpose, a first hydroalkoxylation reaction with MeOH as nucleophile was performed. The GC analysis of the reaction crude after 3 h evidenced the formation of the corresponding methyl ethers in high yields (89 % overall yield). A large excess of ethanol was then added to this catalytic mixture followed by stirring overnight at 80 °C The GC analysis of the resulting crude reaction mixture evidenced the formation of the corresponding ethyl ethers from the methyl ethers with a high conversion.

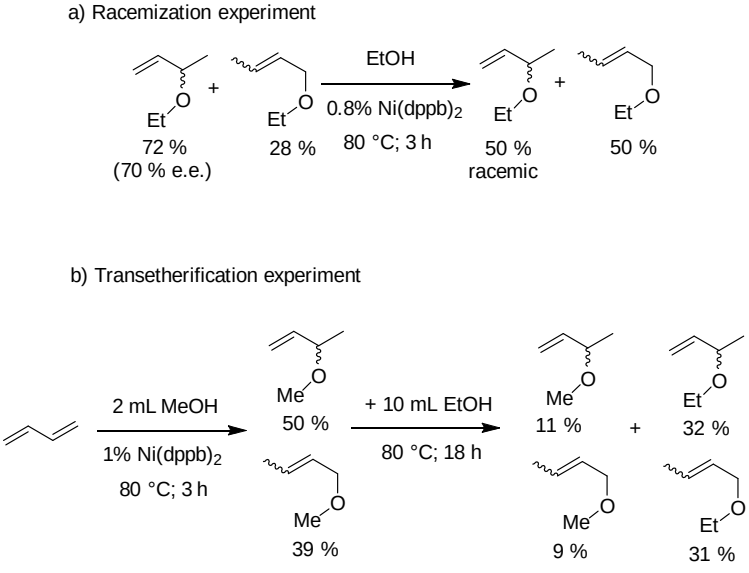

-

Scheme 6. Reversibility of the reaction: The racemization of an enantio-enriched branched butenyl ether and the transetherification experiment.

Density functional theory (DFT) calculations have been employed to probe the mechanism of these Ni-catalysed hydroalkoxylation reactions. The experimental observations suggest a

cycle based on Path B in Scheme 2, i.e. via initial formation of [(P⌒P)Ni(0)(butadiene)] adducts and proceeding via allylic intermediates. In the following, different mechanistic possibilities will initially be explored for the [(dppmb)Ni(0)(*trans*-butadiene)] system, with protonation to give a *syn*-methylallyl intermediate. This will then undergo C-O bond formation via nucleophilic attack at the C^3 position to form a branched ether product. The computational study employed the BP86 functional for all geometry optimizations which also included the effects of methanol solvent via the PCM approach. The resultant free energies were corrected via single point calculations with the ωB97xD functional including methanol solvation and using the def2-tzvp basis set. The full dppmb ligand was used in the calculations, this being preferred to the more conformationally flexible dppb ligand. Similarly, methanol was used as the nucleophile source rather than the ethanol used experimentally. Full computational details are provided in the ESI.

The chemical model employed in the calculations needs some comment as the protonation of the coordinated butadiene in [(dppmb)Ni(0)(*trans*-butadiene)] may occur in either an intramolecular or an intermolecular fashion to generate two possible allylic intermediates formulated either as a Ni-alkoxide complex (**$B_{int\text{-}syn(b)}$**, similar to chloride complexes **2** and **3**) or as an ion-pair featuring a Ni-allyl cation and free methoxide (**$B_{ext\text{-}syn(b)}$**, see Scheme 7). The subsequent C-O bond formation can then also proceed via either an internal or an external attack at the C^3 position to form the branched butenyl ether product (and thus designated (b) in the labeling scheme). Comparing these pathways is challenging due to the formal charge separation present in **$B_{ext\text{-}syn(b)}$** but lacking in **$B_{int\text{-}syn(b)}$**. To address this we have employed a model with three methanol molecules that are H-bonded to give a $(MeOH)_3$ cluster (Scheme 7). Participation of the central methanol in the protonation and (as methoxide) subsequent C-O bond formation steps then allows for a tetrahedral environment to be maintained around the reacting oxygen through a combination of covalent and H-bonding. The use of an extended basis set should also aid the description of the free anion.

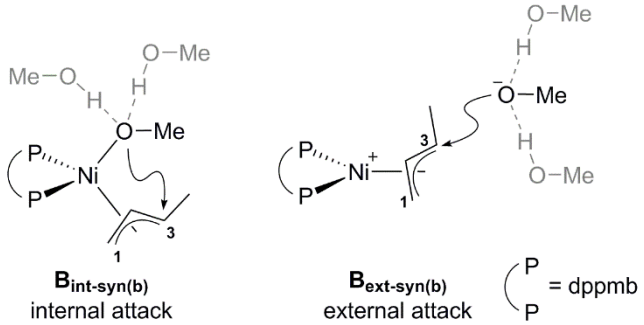

$B_{int\text{-}syn(b)}$ internal attack **$B_{ext\text{-}syn(b)}$** external attack

Scheme 7. Model used in the calculations, illustrated with alternative forms of allyl intermediate **B**.

Computed reaction profiles using this model for both the internal and external mechanisms are shown in Figure 4 where free energies are reported relative to the combined energies of [(dppmb)Ni(0)(η^2-*trans*-butadiene)] and the $(MeOH)_3$ cluster computed separately and set to 0.0 kcal/mol.[27] Starting with precursor **$A_{ext\text{-}trans}$** at +4.5 kcal/mol the external protonation of butadiene proceeds via **$TS(A\text{-}B)_{ext\text{-}trans}$** with a barrier of 13.5 kcal/mol to give the ion-pair **$B_{ext\text{-}syn(b)}$**.[28] The computed geometry of **$TS(A\text{-}B)_{ext\text{-}trans}$** is displayed in Figure 5 and shows the transferring hydrogen H^1 to be approximately midway between O^1 and C^4 (the pendant terminal carbon) along with a Ni···C^3 distance of 2.53 Å.

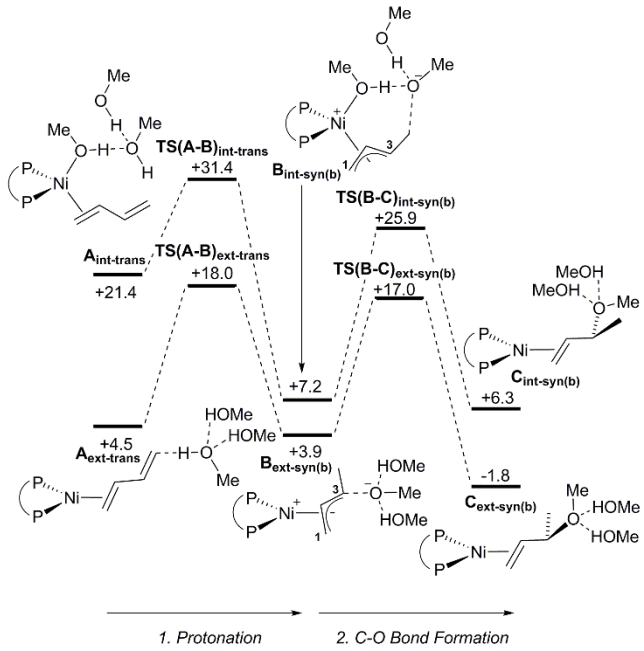

Figure 4. Computed reaction profiles (kcal/mol, ωB97xD in methanol) for formation of 3-methoxybut-1-ene via the external and internal attack pathways at [(dppmb)Ni(0)(η^2-*trans*-butadiene)]. C-O bond formation via external nucleophilic attack at C^1 has a transition state at +16.9 kcal/mol; see text and ESI for details.

This generates a *syn*-methylallyl ligand in **$B_{ext\text{-}syn(b)}$** at +3.9 kcal/mol in which the Ni-C^3 distance has shortened to 2.15 Å. A methoxide anion is now in a position to effect a nucleophilic attack at C^3, and this occurs via **$TS(B\text{-}C)_{ext\text{-}syn(b)}$** at +17.0 kcal/mol (O1···C3 = 2.26 Å, Ni···C3 = 2.58 Å, Figure 5). This forms **$C_{ext\text{-}syn(b)}$** (-1.9 kcal/mol) in which the branched butenyl ether is bound in an η^2-fashion. Hydroalkoxylation via this intermolecular mechanism therefore has an overall barrier of 18.0 kcal/mol, corresponding to the initial H^+ transfer step and is computed to be slightly exergonic (ΔG = -1.9 kcal/mol).

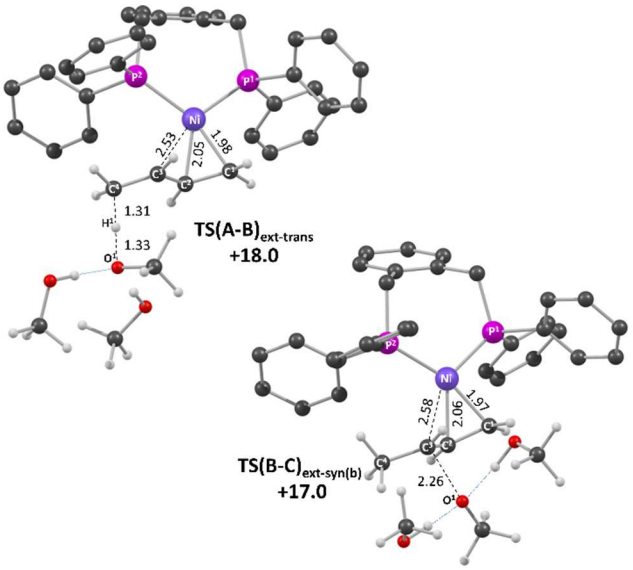

Figure 5. Computed structures of **TS(A-B)$_{ext\text{-}trans}$** and **TS(B-C)$_{ext\text{-}syn(b)}$** with selected distances in Å and relative free energies in kcal/mol. Phosphine H atoms omitted for clarity.

The alternative intramolecular mechanism initiates from a 4-coordinate methanol adduct, **A$_{int\text{-}trans}$**, which has a computed free energy of +21.4 kcal/mol. The subsequent intramolecular H^+ transfer step has a modest barrier of only 10.0 kcal/mol, but this still places **TS(A-B)$_{int\text{-}trans}$** 13.4 kcal/mol above **TS(A-B)$_{ext\text{-}trans}$**. The transition state for C-O bond formation, **TS(B-C)$_{int\text{-}syn(b)}$**, is also 8.9 kcal/mol higher than the equivalent process via **TS(B-C)$_{ext\text{-}syn(b)}$**. A clear preference for the intermolecular pathway is therefore computed. Full details of all structures involved in the intramolecular process, as well as details of the alternative pathways that were considered, are provided in the ESI.

The favoured external pathway defined above results in the formation of the branched butenyl ether. However, C-O bond formation via external nucleophilic attack at C^1 is also possible and would give the linear product. A transition state for this process was located at +16.9 kcal/mol, but as this lies within 0.1 kcal/mol of **TS(B-C)$_{ext\text{-}syn(b)}$** this would imply little l:b kinetic selectivity using this *syn*-methylallyl intermediate.

We have also considered reaction via [(dppmb)Ni(0)(η^2-*cis*-butadiene)] starting from the adduct **A$_{ext\text{-}cis}$** at +7.6 kcal/mol (see Figure 6, where now only the lower energy external pathway is considered). Protonation at C^4 proceeds via **TS(A-B)$_{ext\text{-}cis}$** at +17.3 kcal/mol and forms the *anti*-methylallyl intermediate **B$_{ext\text{-}anti(b)}$**. Nucleophilic attack at C^3 yields the branched butenyl ether product via **TS(B-C)$_{ext\text{-}anti(b)}$** at +14.7 kcal/mol, whereas the alternative attack at C^1 entails a transition state at +18.5 kcal/mol. The overall barrier for reaction from [(dppmb)Ni(0)(η^2-*cis*-butadiene)] is therefore 17.3 kcal/mol and is thus slightly more accessible than that from [(dppmb)Ni(0)(η^2-*cis*-butadiene)] ($\Delta G^{\ddagger}$ = +18.0 kcal/mol). Moreover, once formed, the *anti*-methylallyl intermediate presents a clear kinetic preference for formation of the branched butenyl ether product.

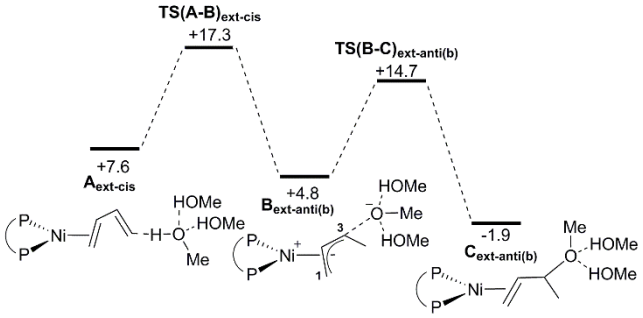

Figure 6. Computed reaction profile (kcal/mol, ωB97xD in methanol) for formation of 3-methoxybut-1-ene from [(dppmb)Ni(0)(η^2-*cis*-butadiene)] via the external pathway. External nucleophilic attack at C^1 has a transition state at +18.5 kcal/mol; see text and ESI for details.

Experimentally, the branched product does dominate at shorter timescales (e.g. l:b ratio = 20:80 after 3 hours), however, over longer periods the observed l:b ratio tends to a 50:50 mixture. Computationally, the branched isomer of the butenyl ether product formed with methanol is computed to be slightly more stable than its linear form, by 0.4 kcal/mol; however with ethanol the two are found to be equi-energetic in agreement with the formation of a 50:50 mixture of both products (see Scheme 8). The overall hydroxylation reactions are also computed to be only marginally exergonic and this, along with the modest overall barriers for the various hydroalkoxylation processes, is consistent with the reversibility observed experimentally. This reversibility explains the racemization depicted in scheme 6. The allylic ether is prone to react with low valent Ni(0) species according to an oxidative addition thus generating a cationic allylic nickel intermediate.[29] As the allylic moiety rapidly interconverts (and the dppb is not chiral), the product is finally racemized after nucleophilic attack of the alkoxide (figure 4). The trans-etherification reaction also proceeds according to a similar mechanism that involves a cationic allylic nickel intermediate. In the presence of a large excess of ethanol (see the trans-etherification experiment of Scheme 6), the methoxy group is exchanged with the ethoxy group of ethanol thus generating ethyl ethers from the initially formed methyl ethers.

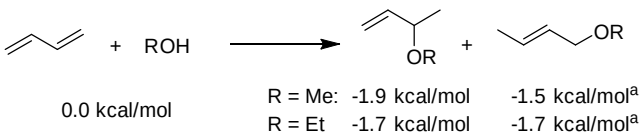

[a]*cis*-isomer at -0.2 kcal/mol (R = Me) and -0.3 kcal/mol (R = Et)

Scheme 8. Computed energetics for the hydroalkoxylation of *trans*-butadiene.

The overall catalytic cycle for the hydroalkoxylation reaction is summarized in Scheme 9. Addition of the chelating phosphines (P⌒P = dppb or dppmb) to [Ni(0)(cod)$_2$] leads to the formation of the [(P⌒P)$_2$Ni(0)] precursor complexes. Experimental studies suggest that in the presence of butadiene, displacement of one chelating phosphine occurs to generate a

key intermediate, [(P⌒P)Ni(0)(butadiene)] which then reacts on via allylic intermediates. DFT calculations suggest that a mechanism involving the external protonation of the butadiene ligand is favored and leads to a cationic nickel(II) complex [(P⌒P)Ni(II)(η^3-C_4H_7)]$^+$ with an alkoxide counterion. The latter is stabilized by H-bonding to the alcohol solvent. Nucleophilic attack by the solvent-stabilized methoxide forms the butenyl ethers as a mixture of linear (CIS and TRANS respectively from the SYN and ANTI allylic isomers) and branched isomers. This last step generates a Ni(0) species that after product displacement by butadiene can enter a new catalytic cycle.

The choice of chelating phosphine is crucial to obtain the selective Ni-catalyzed hydroalkoxylation reaction. In general, a chelating phosphine will tend to impede the coordination of two equivalents of butadiene to the nickel(0) center, thus limiting access to alternative pathways based on butadiene telomerisation. However, the dppmb and dppb appear to be privileged ligands for the C4-hydroalkoxylation reaction: this process fails with dppp or dppe. We postulate that the [(P⌒P)$_2$Ni(0)] precursors are too stable in this case denying phosphine/butadiene exchange and so blocking access to the catalytic cycle. Calculations provide some support for this, the formation of [(P⌒P)Ni(0)(*trans*-butadiene)] (+ free P⌒P) from [(P⌒P)$_2$Ni(0)] (+ free *trans*-butadiene) being more accessible for P⌒P = dppb (ΔG = +10.4 kcal/mol)[30, 31] than for dppp (ΔG = +18.7 kcal/mol) or dppe (ΔG = +17.0 kcal/mol). The computed mechanism also suggests that the use of a protic solvent is also important to stabilize the charged intermediate formed upon diene protonation. Support for this is seen experimentally through the dramatic reduction in the efficiency of the hydroalkoxylation when catalysis was attempted in a non-protic solvent such as toluene (see Table 2).

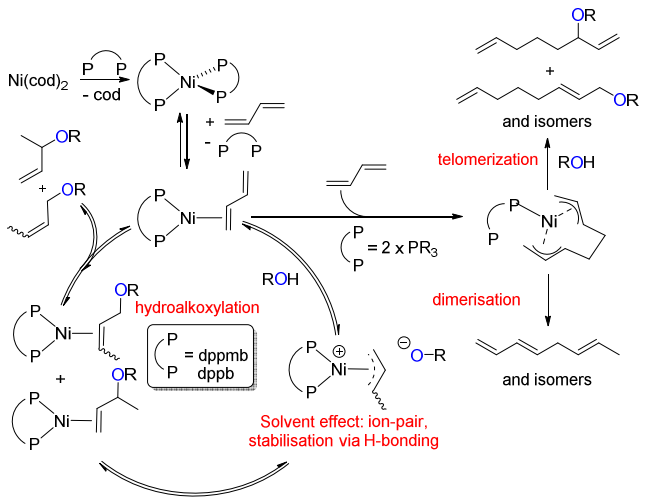

Scheme 9. Proposed catalytic cycle for the Ni-catalysed hydroalkoxylation of butadiene showing potential competing processes.

Comparison with related catalytic systems highlights how control of the reaction outcome can be achieved. Coupling with an additional equivalent of 1,3-butadiene leads to the formation of a bis-allylic intermediate. This species can then react on to form butadiene dimers through an intramolecular proton transfer or products of telomerization (OC8 ethers) in the presence of an alcohol.[29] Here, although the use of alcohols or secondary amines in the presence of phosphine or phosphite has been shown to produce selectively linear dimers, these pathways are occurring only as minor side reactions for the current nickel hydroalkoxylation catalysis.[32] In contrast to its nickel counterparts, palladium-based catalysts show a different behavior and high selectivities toward the products of telomerization are obtained with a wide scope of phosphines and, in particular, monodentate phosphines.

CONCLUSIONS

The mechanism of the Ni-catalyzed hydroalkoxylation reaction of butadiene has been studied through a combination of experimental and computational methods. With the dppb and dppmb co-ligands the reaction proceeds with low catalyst loadings (0,08 mol% Ni) at 80 °C and is particularly efficient when the alcohol is itself used as the solvent. Ni-allyl intermediates are proposed to be likely intermediates in the formation of butenyl ethers and this is supported by the isolation of the related [(P⌒P)Ni(II)(crotyl)Cl] complexes **2** and **3**, both of which are competent catalysts in the presence of sodium ethoxide. The hydroalkoxylation catalysis tolerates both neutral and basic conditions, indicating that Ni-H intermediates are not involved. DFT calculations show that the formation of Ni-allyl intermediates are accessible from the direct protonation of the butadiene moiety in [(P⌒P)Ni(0)butadiene]. This leads to cationic nickel(II) complexes of the type [(P⌒P)Ni(II)(η^3-C_4H_7)]$^+$ with an alkoxide counterion. The latter then acts as a nucleophile to form the butenyl ethers products. Both steps are favored by H-bonding to the protic alcoholic solvent. The computed barriers indicate an initial kinetic preference for the formation of the branched butenyl ether product from an *anti*-methylallyl intermediate. However, the low barriers and small exergonicity of the hydroalkoxylation reaction are consistent with reversible isomerization and racemization processes that lead ultimately to the expected thermodynamic ratio of the butenyl ethers.

ASSOCIATED CONTENT

- Experimental procedures and compound characterization data
- Crystallographic data for compound 2 (CIF)
- Crystallographic data for compound 3 (CIF)
- Computational details and associated references; structures and energies for all computed stationary points; functional testing.

This material is available free of charge via the Internet at http://pubs.acs.org.

AUTHOR INFORMATION

Corresponding Authors

* Mathieu Sauthier : mathieu.sauthier@univ-lille1.fr
*Stuart Macgregor : S.A.Macgregor@hw.ac.uk

Notes

Please direct inquiries regarding X-ray crystallography to frederic.capet@univ-lille1.fr

ACKNOWLEDGMENT

We are grateful to the Region Nord-Pas de Calais for A. Mifleur's fellowship. We acknowledge the Ministery of Research and Technology, the ANR (project H2CAT : ANR-15-CE07-0018-01) and the CNRS for their financial support. We are grateful tot he COST action CARISMA that funded Alexis Mifleur's Short Term Scientific Mission to Heriot-Watt University. We thank Céline Delabre for the analysis assistance.

REFERENCES

(1) *Catalyzed Carbon-Heteroatom Bond Formation*; Yudin, A. K., Eds.; Wiley-VCH: Weinheim, **2011**.

(2) Sauthier, M.; Mortreux, A.; Suisse I.; In *Carbohydrate Chemistry* Rauter A. P.; Lindhorst T.; Queneau Y., Eds.; Royal Society of Chemistry: London, **2014**, p.73.

(3) Behr, A.; Becker, M.; Beckman, T.; Johnen, L.; Leschinski, J.; Reyer, S., *Angew. Chem. Int. Ed.* **2009**, 48, 3598-3614.

(4) Takahashi, S.; Shibano, T.; Hagihara, N., *Tetrahedron. Lett.* **1967**, 8, 2451-2453.

(5) a) Benvenuti, F.; Carlini, C.; Lami, M.; Marchionna, M.; Patrini, R.; Galletti, A. M. R.; Sbrana, G., *J. Mol. Catal. A: Chem.* **1999**, 144, 27-40; b) Tschan, M. J.-L.; García-Suárez, E. J.; Freixa, Z.; Launay, H.; Hagen, H.; Benet-Buchholz, J.; van Leeuwen, P. W. N. M., *J. Am. Chem. Soc.* **2010**, 132, 6463-6473.

(6) a) Clement, N. D.; Routaboul, L.; Grotevendt, A.; Jackstell, R.; Beller, M., *Chem. Eur. J.* **2008**, 14, 7408-7420; b) Mesnager, J.; Lammel, P.; Jeanneau, E.; Pinel, C., *Appl. Catal. A* **2009**, 368, 22-28; c) Grotevendt, A.; Jackstell, R.; Michalik, D., Gomez, M.; Beller, M., *ChemSusChem* **2009**, 2, 63-70.

(7) a) Bohley, R.C.; Jacobsen, G. B.; Pelt, H. L.; Schaart, B. J.; Schenk, M.; van Oeffelen, D. A. G., WO 92/10450 (to DOW Benelux) (1992); b) Mülhaupt, R., *Macromol. Chem. Phys.* **2003**, 204, 289-327; c) Zintl, M.; Rieger, B., *Angew. Chem., Int. Ed.* **2007**, 46, 333-335.

(8) a) Pennequin, I.; Meyer, J.; Suisse, I. ; Mortreux, A., *J. Mol. Catal. A: Chem.* **1997**, 120, 139-142 ; b) Bigot, S.; Lai, J.; Suisse, I.; Sauthier, M.; Mortreux, A.; Castanet, Y., *Appl. Catal. A* **2010**, 382, 181-189.

(9) Grenouillet, P.; Neibecker, D. D.; Poirier, J.; Tkatchenko, I.; *Angew. Chem. Int. Ed.* **1982**, 21, 767-768, *Angew. Chem.* **1982**, 94, 796-797.

(10) a) Mitsubishi Chemical Industries Ltd, FR 2,079,319 (1971); b) Camargo, M.; Dani, P.; Dupont, J.; de Souza, R. F.; Pfeffer, M.; Tkatchenko, I., *J. Mol. Catal. A: Chem.* **1996**, 109, 127-131; c) Bouachir, F.; Grenouillet, P.; Neibecker, D.; Poirier, J.; Tkachenko, I., *J. Organomet. Chem.* **1998**, 569, 203-215.

(11) Dewhirst, K. C., *J. Org. Chem.* **1967**, 32, 1297-1300.

(12) Smutny, E. J., *J. Am. Chem. Soc.* **1967**, 86, 6793-6794.

(13) Patrini, R.; Lami, M.; Marchionna, M.; Benvenuti, F.; Galletti, A. M. R.; Sbrana, G., *J. Mol. Catal. A: Chem.* **1998**, 129, 179-189.

(14) Beger, V. J.; Duschek, C.; Füllbier, H.; Gaube, W., *Journal f. Prakt. Chemie.* **1974**, 316, 26-42.

(15) a) Bigot, S. ; El Alami, M. S. I.; Mifleur, A.; Castanet, Y.; Suisse, I.; Mortreux, A.; Sauthier, M., *Chem. Eur. J.* **2013**, 19, 9785-9788; b) Mifleur, A.; Ledru, H.; Lopes, A.; Suisse, I.; Mortreux, A.; Sauthier, M., *Adv. Synth. and Catal.* **2016**, 358, 1, 110-121; c) Mifleur, A.; Mortreux, A.; Suisse, I.; Sauthier M., *J. mol. Catal. A : Chem.* **2017**, 427, 25-30.

(16) a) Protonation with an imidazolium salt : Clement, N. D.; Cavell, K. J.; Jones, C.; Elsevier C. J., *Angew. Chem. Int. Ed.* **2004**, 43, 1277-1279; b) protonation with an ammonium salt Curtis, C. J.; Miedaner, A.; Ellis, W. W.; DuBois, D. L., *J. Am. Chem. Soc.* **2002**, 124, 1918-1925; c) Miedaner, A.; DuBois, D. L.; Curtis, C. J., *Organometallics* **1993**,12, 299-303; d) protonation with HBF_4 : Rigo, P.; Bressan, M.; Basato, M., *Inorg. Chem.* **1979**, 18, 860-863; e) with HCl : Schunn, R. A., *Inorg. Chem.* **1976**, 15, 208-121.

(17) Tolman, C. A., *J. Am. Chem. Soc.* **1970**, 92, 6777-6783.

(18) a) Pawlas, J.; Nakao, Y.; Kawatsura, M.; Hartwig, J. F., *J. Am. Chem. Soc.* **2002**, 124, 3669-3679; b) Dzhemilev, U. M.; Tolstikov, G. A.; Khusnutdinov, R. I., *Russ. J. Organ. Chem.* **2009**, 45, 957-987.

(19) Shirakura, M.; Suginome, M., *J. Am. Chem. Soc.* **2008**, 130, 5410-5411

(20) Jolly, P. W., *Angew. Chem.,Int. Ed. Eng.* **1985**, 24, 283-295

(21) a) Benn, R.; Jolly, P. W.; Joswig, T.; Mynott, R.; Schick, K.-P., *Z. Naturforsch.* **1986**, *41b*, 640-691; b) Benn, R.; Betz, P.; Goddard, R.; Jolly, P. W.; Kokel, N.; Krüger, C.; Topalović, I., *Z. Naturforsch.* **1991**, *46b*, 1395-1405.

(22) Dreher, E.; Gabor, B.; Jolly, P. W.; Kopiske, C.; Krüger, C.; Limberg, A.; Mynott, R., *Organometallics* **1995**, 14, 1893-1900.

(23) Wilke, G.; Bogdanovic, B.; Hardt, P.; Heimbach, P.; Keim, W.; Kröner, M.; Oberkirch, W.; Tanaka, K.; Steinrücke, E.; Walter, D.; Zimmermann H., *Angew. Chem.* **1966**, *78*, 157-172.

(24) Brunkan, N. M.; Jones, W. D., *J. Organomet. Chem.* **2003**, 683, 77-82.

(25) a) Chaumonnot, A.; Lamy, F.; Sabo-Etienne, S.; Donnadieu, B.; Chaudret, B.; Barthelat, J.-C.; Galland, J.-C.,. *Organometallics* **2004**, 23, 3363-3365; b) see also the following reference for a similar geometry in a related nickel complex with the dppf ligand: Acosta-Ramírez, A.; Muñoz-Hernandez, M.; Jones, W. D.; García, J. J., *J. Organomet. Chem.* **2006**, 691, 3895-3901.

(26) For the synthesis of the enantio-enriched sample, the ethoxylation of butadiene has been performed with the chiral (S)-SEGPHOS ligand. All details are given in the SI.

(27) (dppmb)Ni(butadiene) was computed to be most stable as the η^2-trans isomer, with the η^2-cis and η^4-cis isomers being 1.1 kcal/mol and 3.0 kcal/mol higher in energy, respectively.

(28) Several conformers were located for each intermediate that differ primarily in the relative positions of the butadiene and $(MeOH)_3$ (or related) moieties. Only the lowest energy forms are reported in Figures 4 and 5 and full details of alternative structures are reported in ESI.

(29) A review that details the use of unactivated allylic substrates, this includes the examples with allylic ethers : Butta, N. A.; Zhang, W., *Chem.Soc.Rev.*, **2015**, 44,7929

(30) a) $Ni(dppb)_2$ was used in this analysis as the structure of this species has been determined crystalographically, see Edwards, A.J.; Retboll, M.; Wenger, E., *Acta Crystallogr., Sect. E: Struct. Rep. Online* **2002**, **58**, m375-m377; b) Similarly the structure of $Ni(dppp)_2$ was based on that reported in Davies, S. C.; Duff S. E.; Evans, D.J., *Acta Crystallogr., Sect. E: Struct. Rep. Online* **2005**, **61**, m571-m573.

(31) a) Matusiak, R.; Castanet, Y.; Mortreux, A., *J. Mol. Catal. A: Chemical* **2004**, 217-223; b) Henc, B.; Jolly, P. W.; Salz, R.; Wilke, G.; Benn, R.; Hoffmann, E. G.; Mynott, R.; Schroth, J. N.; Seevogel, K.; Sekutowski, J. C.; Krüger, C., *J. Organomet. Chem.* **1980**, 191, 425-448; c) Brenner, W.; Heimbach, P.; Hey, H.-J.; Müller, W.; Wilke, G., *Liebigs Ann. Chem.* **1969**, 727, 161-182.

(32) a) Heimbach, P., *Angew. Chem. Int. Ed. Engl.* **1973**, 12, 975-989; b) Pittman Jr., C. U.; Smith, L. R., *J. Am. Chem. Soc.*, **1975**, 97, 341-344; c) Denis, P.; Jean, A.; Croizy, J.F.; Mortreux, A.; Petit, F., *J. Am. Chem. Soc.*, **1990**, 112, 1292-1293.

SYNOPSIS TOC (Word Style “SN_Synopsis_TOC”). If you are submitting your paper to a journal that requires a synopsis graphic and/or synopsis paragraph, see the Instructions for Authors on the journal’s homepage for a description of what needs to be provided and for the size requirements of the artwork.